

Magnetic Field Dependence of the Transverse Plasmon in $\text{SmLa}_{0.8}\text{Sr}_{0.2}\text{CuO}_{4-\delta}$

A. Pimenov,¹ A. Loidl,¹ D. Dulić,² D. van der Marel,² I. M. Sutjahja,³ and A. A. Menovsky³

¹*Experimentalphysik V, EKM, Universität Augsburg, 86135 Augsburg, Germany*

²*Laboratory of Solid State Physics, Materials Science Centre, 9747 AG Groningen, The Netherlands*

³*Van der Waals-Zeeman Instituut, University of Amsterdam, The Netherlands*

(Received 15 July 2001; published 5 October 2001)

The magnetic field and temperature dependence of the transverse and longitudinal plasmons in $\text{SmLa}_{0.8}\text{Sr}_{0.2}\text{CuO}_{4-\delta}$ have been investigated. A transition between a vortex-glass and a vortex-liquid regime, which revealed different field dependencies of the resonance frequencies, could be clearly observed. The positions and the spectral weights of the plasmons were successfully described using the multilayer model [Phys. Rev. B **64**, 024530 (2001)], which takes the compressibility of the electronic liquid into account. The absolute value of the compressibility is close to that of a two-dimensional noninteracting electron gas.

DOI: 10.1103/PhysRevLett.87.177003

PACS numbers: 74.25.Gz, 74.50.+r, 74.72.Dn

The Josephson coupling of the CuO_2 layers in the high-temperature superconductors leads to the appearance of a plasma resonance (JPR) along the c axis [1]. The frequency of this resonance is determined by the strength of the Josephson coupling between the layers and is directly connected to the c -axis penetration depth. The magnetic field and temperature dependence of the JPR have been intensively investigated during the past years, providing important information on the c -axis transport and on the vortex dynamics [2–5].

Additional plasma resonances were predicted [6] for systems with two different coupling constants between the CuO_2 layers. For such systems two longitudinal modes and a transverse plasma mode are expected. The transverse excitation couples directly to the electromagnetic radiation and can therefore be observed as a peak in the real part of the optical conductivity. To explain the appearance of transverse plasma oscillations a simple model with alternating coupling constants (multilayer model) has been proposed by van der Marel and Tsvetkov [6].

The investigation of the transverse plasma has proved to be difficult in YBaCuO [7] and BiSrCaCuO [8] because the characteristic maxima overlap with the phonon resonances. In contrast, the plasma frequencies of $\text{SmLa}_{1-x}\text{Sr}_x\text{CuO}_{4-\delta}$ [9] are shifted down to the submillimeter frequency range and therefore can be well separated from the phonons. Recently, several groups reported the observation of one transverse and two longitudinal plasmons in single crystalline $\text{SmLa}_{1-x}\text{Sr}_x\text{CuO}_{4-\delta}$ [10–12] and $\text{Nd}_{1.4}\text{Sr}_{0.4}\text{Ce}_{0.2}\text{CuO}_{4-\delta}$ [11]. However, detailed comparison between the experimental data and the multilayer model predictions revealed substantial discrepancies concerning the position and the spectral weight of the transverse plasmon [10,11]. It has been proposed [13] that the electronic compressibility should be taken into account to bring theory and experiment to better agreement. And, indeed, the extended version of the multilayer model including electronic compressibility [13] was able to

successfully reproduce the position and amplitude of the transverse plasmon [12].

In this paper we present the magnetic field and temperature dependencies of the transverse and longitudinal plasmons in a single crystal of $\text{SmLa}_{0.8}\text{Sr}_{0.2}\text{CuO}_{4-\delta}$ (SmLSCO). The extended version of the multilayer model [13] has been applied to describe the observed spectra. We analyze the dependences of the model parameters with special attention to the electronic compressibility, which in the first approximation may be expected to be independent of magnetic field and temperature.

The single crystals of SmLSCO were grown using a four-mirror image furnace, as described previously [12]. The crystal showed a superconducting transition at $T_c = 16$ K with the transition width of 2 K. A thin ac -oriented plate of the size $\sim 3 \times 4$ mm² was cut from the original crystal and polished to a thickness of $\delta \approx 120$ μm by diamond paste. The transmittance measurements in the submillimeter-wave range were performed using a coherent source spectrometer [14]. Different backward-wave oscillators (BWO's) have been employed as monochromatic and continuously tunable sources covering the range from 5 to 30 cm⁻¹. The Mach-Zehnder interferometer arrangement has allowed the measurement of both the intensity and the phase shift of the wave transmitted through the sample. Using the Fresnel optical formulas for the complex transmission coefficient of a plane-parallel sample, the complex conductivity has been determined directly from the measured spectra. Because of a high degree of the polarization of the radiation, the spectra could be, in principle, measured along both the a and c axes. However, due to the high conductivity of SmLSCO within the CuO_2 planes, the sample was completely opaque for the $\vec{e} \parallel a$ axis (\vec{e} is the ac -electric field of the incident radiation). The anisotropy could be measured solely for room temperature as $\sigma_a/\sigma_c \approx 19 \pm 3$.

The magnetic field $B \leq 7$ T has been applied along the c axis by using a superconducting split-pair magnet

equipped with Mylar windows. The experiments in the magnetic field were performed using the field sweeping (FS) conditions [3]. Within the FS conditions the actual field in the sample may deviate from the external field by the value determined by the Bean critical field [15] $H_c = J_c \delta / 2$, where J_c is the critical current density and δ is the sample thickness. From the magnetization measurements the Bean critical field has been determined to be $H_c \approx 500$ Oe at $T = 2$ K, which corresponds to $J_c \approx 6.6 \times 10^4$ A/cm². The demagnetization effects can be neglected because of the thin-plate geometry of the experiment.

Figure 1 shows examples of transmittance and phase shift spectra of SmLSCO along the c axis above and below the superconducting transition. The overall frequency dependence of the data is dominated by the interference fringes due to the relative transparency of the sample along the c axis. In the normally conducting state ($T = 20$ K) the interference maxima are seen at about $\nu_1 = 10.6$ cm⁻¹ and $\nu_2 = 21.3$ cm⁻¹, from which the c -axis dielectric constant, $\epsilon_c = 15.2$, can be directly estimated via $2\delta\epsilon_c^2 = m/\nu_{\max}$. Here $m = 1, 2$ is an integer. The measured curves in Fig. 1 are strongly modified in the superconducting state: both transmittance and phase shift are suppressed at low frequencies due to the growth of the imaginary part of the complex conductivity $\sigma^* = \sigma_1 + i\sigma_2$. Most importantly, two new effects can be directly observed in the experimental transmittance data as an additional maximum at $\nu_I \approx 6.7$ cm⁻¹ and a minimum at $\nu_T \approx 12.1$ cm⁻¹. The first feature corresponds to the (low-lying) longitudinal plasmon and is also seen as a zero crossing of the phase shift. The

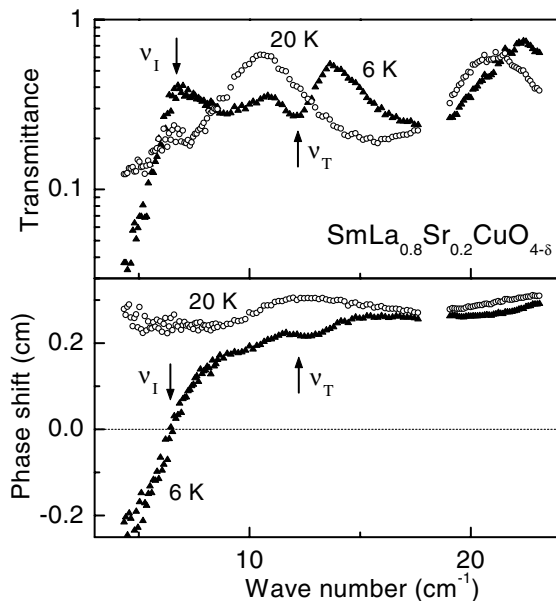


FIG. 1. Transmittance and phase shift spectra of SmLa_{0.8}Sr_{0.2}CuO_{4- δ} along the c axis in zero magnetic field. The arrows indicate the positions of the transverse (ν_T) and of the low-lying longitudinal plasmons (ν_K).

second feature corresponds to a transverse plasmon and is characterized by a minimum in transmittance and a smooth step in the phase shift. The second longitudinal plasmon ($\nu_K \approx \nu_T + 0.2$ cm⁻¹) is not seen in the transmittance spectra because it strongly overlaps with the transverse resonance.

The evaluation of the complex conductivity from the transmittance and phase shift removes the interference fringes from the spectra because they are automatically included in the Fresnel expressions. The resulting conductivity (σ_1) and the loss function ($\text{Im}[1/\epsilon^*]$) are represented in Fig. 2 for different magnetic fields along the c axis. The complex dielectric function is given by $\epsilon^* = \epsilon_1 + i\epsilon_2 = i\sigma^*/\epsilon_0\omega$, where ϵ_0 is the permittivity of free space and $\omega = 2\pi\nu$ is the angular frequency. The transverse plasmon is clearly seen in the lower frame of Fig. 2 as a maximum of σ_1 . The longitudinal plasmons cannot be observed in the real part of the conductivity because they do not lead to the absorption of the electromagnetic radiation. Instead, they can be observed as peaks in the loss function.

Figure 3 represents the magnetic field dependence of the plasma resonances in SmLSCO. The frequency of the transverse plasmon was determined by the peak positions in σ_1 and the frequency of the longitudinal plasmons was derived from the maxima of the loss function. For high fields and high temperatures the low-lying longitudinal plasmon was shifted to low frequencies, outside the range of our experiment. In that case, the resonance frequency was obtained as the zero crossing of ϵ_1 , assuming that in the superconducting state the usual low-frequency relation holds: $\epsilon_1 \propto -1/\nu^2$.

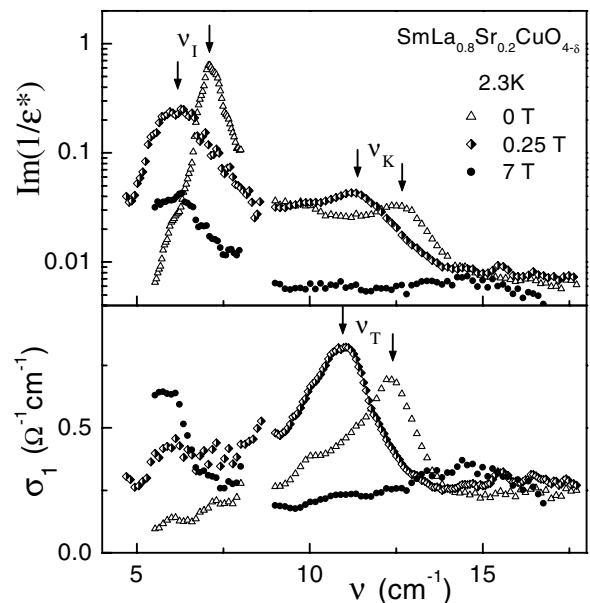


FIG. 2. Real part of the complex conductivity σ_1 and loss function $\text{Im}(1/\epsilon^*)$ of SmLa_{0.8}Sr_{0.2}CuO_{4- δ} along the c axis for different magnetic fields at 2.3 K. The transverse plasmon ν_T shows up as a peak in σ_1 , the longitudinal plasmons $\nu_{I,K}$ show up as peaks in $\text{Im}(1/\epsilon^*)$.

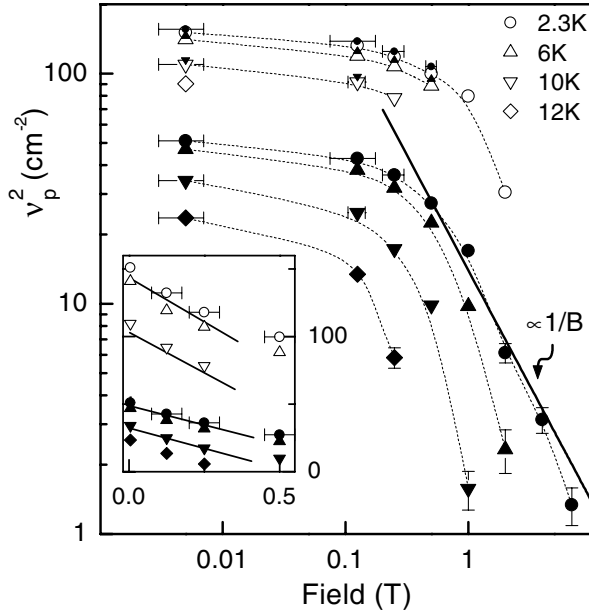


FIG. 3. Magnetic field dependence of the (squared) c -axis plasmons in $\text{SmLa}_{0.8}\text{Sr}_{0.2}\text{CuO}_{4-\delta}$: open symbols, transverse plasmon; large and small closed symbols, longitudinal plasmons. The thin dashed lines are guides to the eye. The thick solid line indicates a $1/B$ field dependence. The inset represents the data on the linear scale.

For all resonances presented in Fig. 3 the field dependence can be clearly separated in two regimes: a low-field region with a weak-field dependence below 0.1–1.0 T and a high-field regime, for which an approximate dependence $\nu_p^2 \propto 1/B$ is applicable. We identify therefore the high-field region as a vortex-liquid state, in which both theoretically [16] and experimentally [3–5] the plasma frequency has been shown to behave as $\nu_p^2(B, T)/\nu_p^2(0) \propto B^{-1}T^{-1}$.

In addition, the inset of Fig. 3 represents the low-field dependence of the plasma frequencies on the linear scale. From this presentation the linear field dependence of ν_p^2 in low magnetic field becomes evident. At low fields the regime of isolated vortices is expected to be applicable and no field dependence of the plasma frequency is expected in zeroth order approximation. However, taking into account thermal fluctuation and pinning disorder, a linear correction of the squared plasma frequency is expected theoretically [17] and has been recently observed [18] in $\text{Tl}_2\text{Ba}_2\text{CaCu}_2\text{O}_8$ using the JPR technique. However, we note that the theoretical considerations were carried out for the system with a single Josephson coupling between the CuO_2 layers. In the zeroth order approximation, we also expect the same magnetic field dependencies for a system with two coupling constants such as SmLSCO .

The upper panels of Fig. 4 represent the dielectric contribution of the transverse plasmon $\Delta\epsilon_T = \omega_T^2/\omega_p^2$, which may be obtained either by integrating the area under the resonance in σ_1 via $\omega_p^2 = \frac{2}{\pi\epsilon_0} \int \sigma_1(\omega) d\omega$ (Fig. 2) or by fitting a conventional oscillator model to the complex conductivity. Both procedures lead to similar results. A reliable analysis of the spectra could be carried

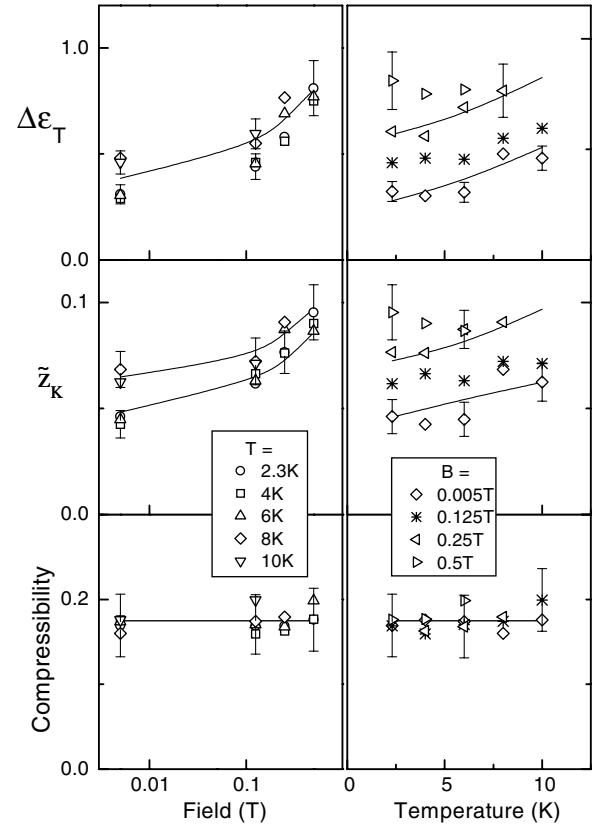


FIG. 4. Upper panels: magnetic field (left) and temperature (right) dependence of the dielectric contribution of the transverse plasmon in $\text{SmLa}_{0.8}\text{Sr}_{0.2}\text{CuO}_{4-\delta}$. Middle panels: field (left) and temperature (right) dependence of the weight factor $\tilde{z}_K = 1 - \tilde{z}_I$ in SmLSCO , obtained according to the multilayer model [6,13]. Lower panels: electronic compressibility $\gamma = \epsilon_0\epsilon_\infty/(de^2Kn^2)$ in SmLSCO . The lines are guides to the eye.

out for $B \leq 0.5$ T only, which explains the somewhat limited range of data in Fig. 4. As demonstrated by the upper left panel of Fig. 4, the magnetic field strongly influences the dielectric contribution of the transverse plasma: $\Delta\epsilon_T$ increases by a factor of 2 between $B \approx 0$ and $B = 0.5$ T. The field enhancement of $\Delta\epsilon_T$ leads to the nonconservation of the transverse spectral weight $\omega_p^2 = \Delta\epsilon_T\omega_T^2$. According to Fig. 3, ω_T^2 is reduced by a factor of 1.5 at $B = 0.5$ T, which does not compensate the doubling of the dielectric contribution and indicates a $\sim 30\%$ enhancement of the transverse spectral weight in the magnetic field of 0.5 T. The temperature dependence of the dielectric contribution $\Delta\epsilon_T(T)$ is shown in the upper right panel of Fig. 4. As in the case of the field dependence, the data indicate a weak increase with temperature.

Finally, we discuss the results within the frame of the multilayer model [13]. In this model the dielectric constant of a layer with two different coupling constants is given by

$$\frac{\epsilon_\infty}{\epsilon^*(\nu)} = \frac{\tilde{z}_I\nu^2}{\nu^2 - \nu_I^2 + i\nu g_I} + \frac{\tilde{z}_K\nu^2}{\nu^2 - \nu_K^2 + i\nu g_K}, \quad (1)$$

where ν_I^2 and ν_K^2 are low- and high-frequency longitudinal plasma frequencies, g_I and g_K are the corresponding damping factors, and $\epsilon_\infty \approx 16$ is the high-frequency

dielectric constant. The transverse plasma frequency ν_T is given by $\nu_T^2 = \tilde{z}_K \nu_I^2 + \tilde{z}_I \nu_K^2$. Here \tilde{z}_K and \tilde{z}_I are the weight factors of both longitudinal plasmons, which are connected as $\tilde{z}_K + \tilde{z}_I = 1$. The weight factors are obtained via [13]

$$\tilde{z}_K = \frac{1}{2} - \frac{2\gamma(z_K z_I + \gamma)}{z_K z_I + 2\gamma + 4\gamma^2} \frac{\nu_K^2 + \nu_I^2}{\nu_K^2 - \nu_I^2} + \frac{(z_K - z_I)(z_K z_I + 2\gamma)}{2(z_K z_I + 2\gamma + 4\gamma^2)} \sqrt{1 - \frac{4(2\gamma)^2 \nu_K^2 \nu_I^2}{(\nu_K^2 - \nu_I^2)^2}}. \quad (2)$$

Here $z_{K,I}$ are the unrenormalized weight factors which are directly obtained from the relative distances $d_{1,2}$ between the corresponding layers in SmLSCO $z_{K,I} = d_{1,2}/(d_1 + d_2)$. This leads to $z_K \approx z_I \approx 0.5$, because $d_1 \approx d_2$. A correction due to the lattice polarizability, characterized by the dielectric constants of the layers, gives [12,13] $z_K = 1 - z_I \approx 0.43 \pm 0.08$.

Despite its relative complexity, the advantage of Eq. (2) is that it contains only one unknown parameter γ which is inversely proportional to the two-dimensional electronic compressibility (K), $\gamma = \varepsilon_0 \varepsilon_\infty / (de^2 K n^2)$. Here n is the electron density and $d = 12.56 \text{ \AA}$ is the lattice constant along the c axis. The frequencies ν_K^2, ν_I^2 and the weight factor \tilde{z}_K are measured in the experiment, while the starting weight factors $z_{K,I}$ are obtained from structural considerations.

The data, presented in Fig. 3 and in the upper panel of Fig. 4, are already sufficient to determine all of the parameters of the model, because the dielectric contribution of the transversal plasma $\Delta\varepsilon_T$ can be obtained from Eq. (1) and is given by $\Delta\varepsilon_T = \varepsilon_\infty \tilde{z}_K \tilde{z}_I (\nu_K^2 - \nu_I^2)^2 / \nu_T^4$. The values of the weight factors can be obtained from known resonant frequencies and the dielectric contribution. However, equivalent results were obtained by directly fitting the experimental spectra using Eq. (1).

The middle panels of Fig. 4 show the weight factor of the high-frequency plasmon in SmLSCO as a function of the temperature and the magnetic field. The weight factor \tilde{z}_K reveals the dependencies, which are similar to that of $\Delta\varepsilon_T$ in the upper panel: a pronounced increase in the magnetic field and a much weaker but still visible increase as a function of temperature.

A striking result of this work is shown in the lower panels of Fig. 4, which represent the electronic compressibility of SmLSCO. The compressibility reveals neither field nor temperature dependence in the presented range. As a matter of fact, in first approximation it can be expected that the compressibility $Kn^2 = \partial n / \partial \mu$, where μ is the chemical potential, is independent of field and temperature. This strongly supports the idea that γ indeed is the reason for the deviation of the the simple version of the multilayer model [6] from experimental data [10–12]. From the data

of Fig. 4 we obtain $Kn^2 = 0.6 \pm 0.2 \text{ eV}^{-1}$ per Cu atom. A discrepancy in the absolute value of Ref. [12] ($Kn^2 = 1.1 \text{ eV}^{-1}$) is due to the difference in the high-frequency dielectric constant, which has been adopted for calculations. We note further that the electronic compressibility of the two-dimensional electronic gas depends upon the effective mass only, $Kn^2 = \partial n / \partial \mu = m_{\text{eff}} / (\pi \hbar^2)$, from which the effective mass may be estimated: $m_{\text{eff}} = 0.95 m_e$.

In conclusion, we have measured the magnetic field and temperature dependencies of the longitudinal and transverse plasmons in $\text{SmLa}_{0.8}\text{Sr}_{0.2}\text{CuO}_{4-\delta}$. The field dependence of the resonance frequencies ν_p^2 reveals two different regimes. In the low-field region $B < 0.1\text{--}1.0$, which we identify as a vortex-glass regime, ν_p^2 linearly depends upon field. For higher magnetic fields, ν_p^2 are much more strongly suppressed, which may be approximated by $\nu_p^2 \propto B^{-1.25}$ and is close to $\nu_p^2 \propto 1/B$ known from the theory of the vortex-liquid state. The full experimental data set was successfully described by the multilayer model by van der Marel and Tsvetkov [13], which includes the electronic compressibility to correctly obtain the frequency and the spectral weight of the transverse plasmon. The most surprising result is the field and temperature *independence* of the compressibility, with an absolute value close to that of a two-dimensional noninteracting electron gas.

We thank A. A. Tsvetkov and Ch. Helm for useful discussions. This work was supported by the BMBF via Contract No. 13N6917/0-EKM.

- [1] M. Tachiki, T. Koyama, and S. Takahashi, in *Coherence in High Temperature Superconductors*, edited by G. Deutscher and A. Revcolevschi (World Scientific, Singapore, 1995), p. 371.
- [2] O. K. C. Tsui *et al.*, Phys. Rev. Lett. **73**, 724 (1994).
- [3] Y. Matsuda *et al.*, Phys. Rev. Lett. **78**, 1972 (1997).
- [4] T. Shibauchi *et al.*, Phys. Rev. Lett. **83**, 1010 (1999).
- [5] M. B. Gaifullin *et al.*, Phys. Rev. Lett. **84**, 2945 (2000).
- [6] D. van der Marel and A. A. Tsvetkov, Czech. J. Phys. **46**, 3165 (1996).
- [7] D. Munzar *et al.*, Solid State Commun. **112**, 365 (1999); M. Grüninger *et al.*, Phys. Rev. Lett. **84**, 1575 (2000).
- [8] V. Železný *et al.*, Phys. Rev. B **63**, 060502 (2001).
- [9] H. Shibata and T. Yamada, Phys. Rev. Lett. **81**, 3519 (1998).
- [10] H. Shibata, Phys. Rev. Lett. **86**, 2122 (2001).
- [11] T. Kakeshita *et al.*, Phys. Rev. Lett. **86**, 4140 (2001).
- [12] D. Dulić *et al.*, Phys. Rev. Lett. **86**, 4144 (2001).
- [13] D. van der Marel and A. A. Tsvetkov, Phys. Rev. B **64**, 024530 (2001).
- [14] A. A. Volkov *et al.*, Infrared Phys. **25**, 369 (1985).
- [15] C. P. Bean, Rev. Mod. Phys. **36**, 31 (1964); E. H. Brandt, Rep. Prog. Phys. **58**, 1465 (1995).
- [16] A. E. Koshelev, Phys. Rev. Lett. **77**, 3901 (1996).
- [17] L. N. Bulaevskii *et al.*, Phys. Rev. B **61**, R3819 (2000); A. E. Koshelev, L. I. Glazman, and A. I. Larkin, Phys. Rev. B **53**, 2786 (1996).
- [18] D. Dulić *et al.*, Phys. Rev. Lett. **86**, 4660 (2001).